Biochimica et Biophysica Acta 1838 (2014) 244–253

Contents lists available at ScienceDirect

Biochimica et Biophysica Acta

journal homepage: www.elsevier.com/locate/bbamem

Review

The sodium/iodide symporter: State of the art of its molecular characterization

Elisabeth Darrouzet [a,b,c,*,1], Sabine Lindenthal [b,c,d,1], Didier Marcellin [a,b,c], Jean-Luc Pellequer [e], Thierry Pourcher [b,c,d]

[a] SBTN, bât 170, centre de Marcoule, BP 17171, 30207 Bagnols sur Cèze CEDEX, France
[b] Laboratoire TIRO, Faculté de médecine, Université de Nice Sophia-Antipolis, 28 Avenue de Valombrose, 06107 Nice CEDEX, France
[c] CAL, TIRO, F-06107 Nice, France
[d] CEA, iBEB, SBTN, TIRO, F-06107 Nice, France
[e] CEA, iBEB, SBTN, LIRM, F-30207 Bagnols sur Cèze, France

ARTICLE INFO

Article history:
Received 6 June 2013
Received in revised form 5 August 2013
Accepted 19 August 2013
Available online 27 August 2013

Keywords:
Sodium/iodide symporter
NIS
SLC5A5
Thyroid
Membrane protein
Structure/function relationship

ABSTRACT

The sodium/iodide symporter (NIS or SLC5A5) is an intrinsic membrane protein implicated in iodide uptake into thyroid follicular cells. It plays a crucial role in iodine metabolism and thyroid regulation and its function is widely exploited in the diagnosis and treatment of benign and malignant thyroid diseases. A great effort is currently being made to develop a NIS-based gene therapy also allowing the radiotreatment of nonthyroidal tumors. NIS is also expressed in other tissues, such as salivary gland, stomach and mammary gland during lactation, where its physiological role remains unclear. The molecular identity of the thyroid iodide transporter was elucidated approximately fifteen years ago. It belongs to the superfamily of sodium/solute symporters, SSS (and to the human transporter family, SLC5), and is composed of 13 transmembrane helices and 643 amino acid residues in humans. Knowledge concerning NIS structure/function relationship has been obtained by taking advantage of the high resolution structure of one member of the SSS family, the *Vibrio parahaemolyticus* sodium/galactose symporter (vSGLT), and from studies of gene mutations leading to congenital iodine transport defects (ITD). This review will summarize current knowledge regarding the molecular characterization of NIS.

Contents

1. Introduction

The iodide uptake ability of thyroid cells has been known for more than a century. However, the molecular identity of the iodide transporter was only determined around fifteen years ago, first in the rat [1], and

* Corresponding author at: SBTN, bât 170, centre de Marcoule, BP 17171, 30207 Bagnols sur Cèze CEDEX, France. Tel.: +33 4 66 79 19 16.
E-mail addresses: elisabeth.darrouzet@cea.fr (E. Darrouzet), sabine.lindenthal@unice.fr (S. Lindenthal), didier.marcellin@cea.fr (D. Marcellin), jean-luc.pellequer@cea.fr (J.-L. Pellequer), thierry.pourcher@unice.fr (T. Pourcher).
[1] Joint first authors.

0005-2736/$ – see front matter © 2013 Elsevier B.V. All rights reserved.
http://dx.doi.org/10.1016/j.bbamem.2013.08.013

then in the human, mouse and pig [2–4]. The protein has been named NIS, for Natrium Iodide Symporter.

NIS is an intrinsic membrane protein belonging to the superfamily of sodium/solute symporters (SSS) and to the human transporter family, SLC5 [5,6]. The protein is found in the basolateral membrane of thyroid follicular cells (as illustrated in Fig. 1) where it mediates efficient iodide uptake from the bloodstream into the thyroid using the sodium gradient generated by Na^+/K^+-ATPase. It makes an essential contribution to thyroid hormone synthesis and, therefore, to the control of human metabolism in general. NIS is a key protein in thyroid regulation and its expression is finely tuned at the transcriptional and post-transcriptional levels [7,8]. Its function also plays a crucial role in the diagnosis and treatment of benign and malignant thyroid diseases [9–12]. Studies are currently underway to better control NIS regulation, which could be useful in many fields including: i) the radiotherapy of thyroid in which NIS expression is low and radioiodine uptake needs to be enhanced [13] and ii) the development of new strategies to decrease thyroid irradiation after accidental radioiodine exposure [14]. A great effort is also being made to develop a NIS-based gene therapy allowing the radiotreatment of nonthyroidal tumors [12,15,16]. For this purpose, efficient gene transfer and protein expression in the targeted host cells are required [17–19] and NIS mutants leading to strong expression of highly active protein with efficient targeting to the plasma membrane are sought.

NIS expression is also found in other cells/tissues, such as salivary gland ductal cells [20,21], breast tissue during lactation [3,22,23], lung airway epithelial cells [24], intestinal enterocytes [25], epithelial and parietal stomach cells [26], placenta [27] and testicular cells [28]. The functional role of the protein in these tissues remains speculative.

This review will summarize current knowledge regarding the molecular characterization of NIS at the functional, biochemical and structural levels.

2. NIS functional characterization

NIS transports one iodide ion along with two sodium ions following the inwardly directed sodium gradient. For the rat NIS, the apparent affinity constants are 30 mM and 30 μM for Na^+ and I^-, respectively, with a turnover rate of more than 36 s^{-1} [29].

Li^+ can also be used as a coupling cation but the transport activity is only about 10% of that obtained with Na^+, while H^+ is barely transported [29]. The following anions are known to be NIS substrates: ClO_3^-, SCN^-, $SeCN^-$, NO_3^-, ReO_4^-, TcO_4^- and to a lower extent Br^- and BF_4^- [29,30] (see Table 1). ClO_4^- has long been considered to be a NIS inhibitor [29,30], but Dohan and colleagues clearly showed that this anion is transported by NIS. Interestingly, the transport is non electrogenic, with a 1:1 stoichiometry [31].

A Na^+-dependent leak (35% of the substrate-induced current) has been described and a model in which one sodium ion binds first has been proposed for the translocation mechanism [29]. The uptake by NIS of either one thiocyanate or one iodide, along with two sodium ions, is accompanied by the transport of 253 or 162 water molecules, respectively [32].

3. NIS topology and biochemical characterization

NIS is composed of 618 amino acids in the rat [1] and mouse [3], and 643 amino acids in the human [2] and pig [4]. Porcine NIS is also present as various isoforms due to alternative splicing of its mRNA at sites that are not present in the human or murine species [4].

The NIS protein carries three N-linked glycosylations (at positions 225, 485 and 497 of the rat sequence), resulting in a mature protein that migrates at an apparent molecular weight of 80–90 kDa. An additional, partially glycosylated form migrating at an apparent molecular weight of 60 kDa can also be seen on SDS-PAGE [33,34]. As shown by Levy et al., NIS glycosylation is not required for the correct targeting of the protein to the plasma membrane but plays a role in protein stabilization and folding [34]. For some tissues, such as stomach or breast, western-blot analyses have also revealed occasional protein species migrating at lower apparent molecular weights. It was concluded that these findings were most probably due to incomplete glycosylation [22,26].

NIS protein topology was first predicted by bioinformatics (hydropathy profile) [1] to form twelve transmembrane helices (TM), but this model has since been modified to a topology with thirteen TM [5]. In the latter model, the N-terminus extremity is extracellular and the C-terminus intracellular. The extracellular localization of the N-terminus was established with a Flag epitope NIS fusion protein and an anti-Flag antibody used on transfected, nonpermeabilized COS cells [34]. A typical N-terminal signal peptide is missing. The intracellular localization of the C-terminus was confirmed by immunocytochemistry [35]. The intracellular C-terminus contains 70 amino acids in the rat and 100 in the human, and represents the longest stretch of amino acid residues predicted to lie outside the membrane. This portion contains numerous potential phosphorylation sites (PKA, PKC, CKII), two of which have been biochemically validated in rat NIS (T575 and S581, [36]). This domain also bears several potential binding sites for regulatory proteins and is predicted by bioinformatics to have few secondary structures, and thus to be intrinsically unstructured.

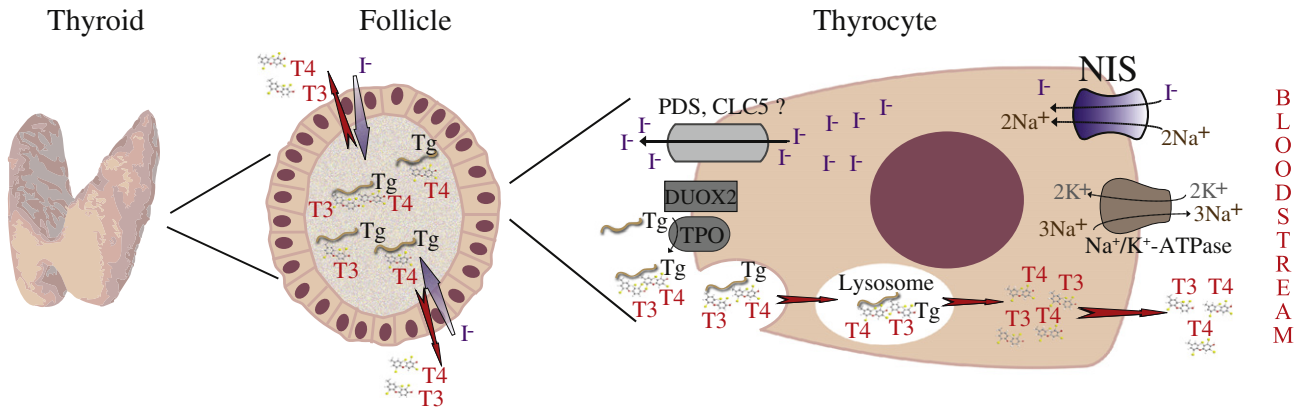

Fig. 1. Schematic representation of iodide metabolism in the thyroid and of the role of NIS. Tg: thyroglobulin. T3 and T4: triiodothyronine and thyroxine hormones, respectively. NIS uses the sodium gradient generated by the Na^+/K^+-ATPase to actively transport iodide into thyrocyte cells. The iodide ions cross the cells and are organified (covalently linked) inside the thyroid follicles by thyroid peroxidase (TPO) onto thyroglobuline tyrosine residues. These iodotyrosines are then coupled to form thyroid hormones. After endocytosis, the iodinated Tg is proteolysed, and the thyroid hormones are released into the bloodstream.

Table 1
Properties of the major anions transported by NIS.

Anion transported	Stoichiometry Na^+/anion	K_m in μM[a]	K_i in μM[a]
I^-	2/1 [29]	33 [29]; 9.7 [31]; 30 [116]; 33 [117] 9/26.4 for hNIS vs. mNIS [43] 132/122 for hNIS vs. rNIS [56]	33.9 [118] 10.3/51.1 for hNIS in COS cells vs. rNIS in FRTL5 [30];
ClO_3^-	≥2/1 [30]	486 [117] 277 at 100 mM Na^+, 1671 at 20 mM Na^+ [29]	131/1368 for hNIS in COS cells vs. rNIS in FRTL5 [30]
SCN^-	≥2/1 [119]	96 [29]; 20–30 [116]; 38 [117]	19.3 [118]; 30 [116] 23.5/33.6 for hNIS in COS cells vs. rNIS in FRTL5 [30];
$SeCN^-$		38 [29]	
NO_3^-		739 [29]; 770 [117]	297 [118]
Br^-			5944/26,250 for hNIS in COS cells vs. rNIS in FRTL5 [30]
ClO_4^-	1/1 [31]	1.5 [31]; 3.9 [117]	1.8 [29]; 1.27 [118]; 2 [116] 0.43/0.62 for hNIS in COS cells vs. rNIS in FRTL5 [30];
ReO_4^-	1/1 [31]	2.3 [31]; 1.9 [117]	3.2 [29]; 1.12/1.22 for hNIS in COS cells vs. rNIS in FRTL5 [30]
TcO_4^-	1/1 [31]		

[a] The values given in this table are illustrative and depend greatly on the experimental conditions (uptake versus electrophysiological measurements, species, cell line, Na^+ concentration used…). See references for details.

The orientation of different loops, and of the N-terminus, was confirmed by introducing specific glycosylation sites into a nonglycosylated variant and by introducing a cysteine residue at position 160 (external loop 2) in an extracellular cysteine-less background and then probing with a sulfhydryl membrane-impermeable reagent [5]. The established model strongly resembles those proposed for other members of the SSS family, including the sodium/galactose symporter for which the three-dimensional structure has been established by Abramson's group [37,38] (see below in the NIS family section for details, and Fig. 5 for a NIS model derived from this structure).

Another feature of membrane proteins, including NIS, is their appearance in different oligomeric forms modulating their maturation, targeting, stability and even function [39,40]. Freeze-fracture electron microscopy with NIS-mRNA-injected *Xenopus* oocytes has strongly suggested that the protein is present in a multimeric form [29]. SDS-PAGE analysis of NIS protein in the thyroid [41,42], in a thyroid-derived cell line [35], and in transfected mammalian cells that transiently [43] or stably [44] express NIS, revealed high-molecular-weight species corresponding to a protein dimer (or oligomer) that was resistant to the strong detergent, SDS. Dai and collaborators suggested that a leucine-zipper motif in TM6 of rat NIS is involved in the dimerization process [1]. However, this motif is not conserved in human, mouse or pig NIS, and this helix is not located at the interface in the crystallographic dimer of vSGLT [37]. A more detailed study of the biochemical characterization of NIS was performed in our laboratory [44]. For the first time, human NIS (hNIS) protein was purified in milligram amounts and a highly enriched, solubilized NIS fraction was analysed by light scattering coupled with size exclusion chromatography. It was shown that this fraction contained different molecular weight NIS species. Only a minority of monomer species (less than three percent) was detected. The majority of NIS species had molecular weights corresponding to those of the dimer and higher multimers [44]. Our group also showed that at least one disulphide bond is formed during dimeric association [44]. The effect of dimerization on NIS function and/or regulation remains to be established.

A NIS fragment of approximately 15 kDa was detected by Castro and colleagues [41] using western blot analysis with NIS-expressing COS-7 cells. This fragment was also identified in various tissues of different species [42,44,45]. Huc-Brandt et al. showed that the fragment from hNIS consists of the 131 C-terminal amino acid residues and, thus, includes the last predicted transmembrane helix (TM13)[44]. Disulphide bonding seems to be involved in its interaction with a higher molecular

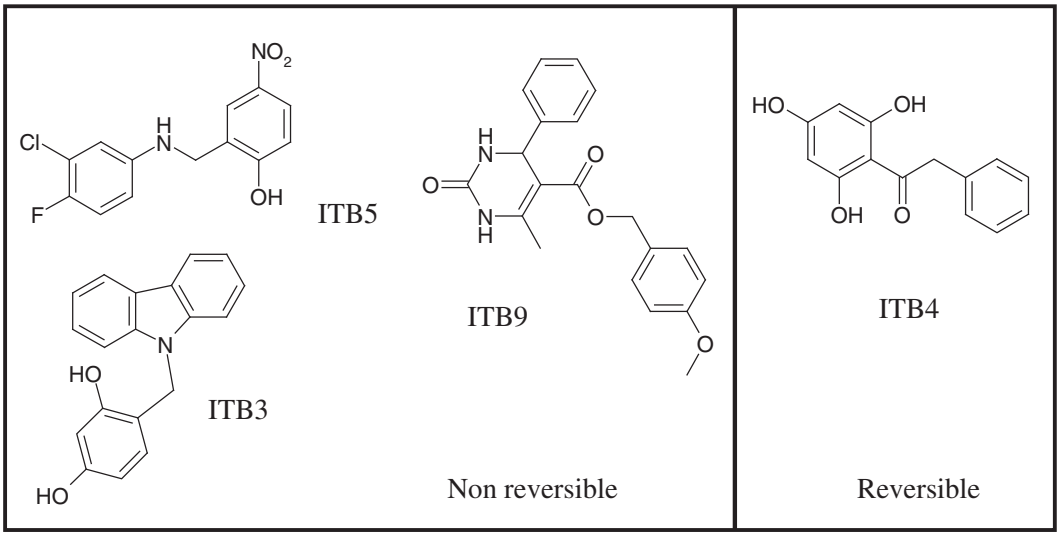

Fig. 2. Inhibitors of NIS. The chemical structures of four potent NIS inhibitors are shown. They are sorted in two groups (reversible and non reversible effects), as detailed by Lindenthal et al. [52].

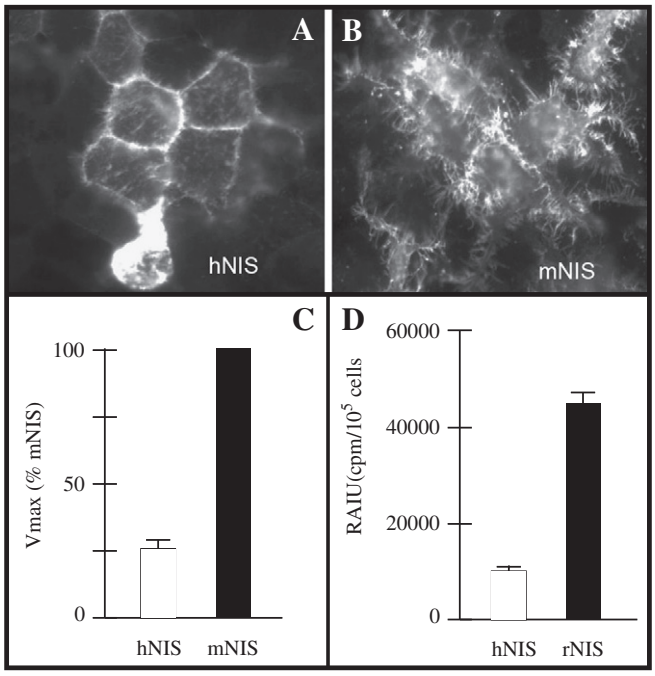

Fig. 3. Characterization of NIS orthologs. Panels A and B show the difference in immunolocalization between human NIS (hNIS) and mouse NIS (mNIS) in transiently transfected HEK cells, as detailed in [43]. Panels C and D display the difference in iodide uptake between human and mouse or rat NIS, respectively, as described by Dayem et al. [43] and Zhang et al. [56].

weight NIS form [44]. Moreover, when the 15 kDa C-terminal fragment is coexpressed with its N-terminal counterpart, a functional symporter is reconstituted. When expressed alone, the N-terminal fragment is found at a very low level, but can be detected in the plasma membrane [44]. Thus, it was concluded that the C-terminal portion is not necessarily required for correct protein targeting. However, no transport activity can be detected with the truncated protein, highlighting an important role of the 15 kDa C-terminal fragment for the transporter function [44]. The genesis of the 15 kDa fragment, and its physiological role, remains unknown.

4. NIS inhibitors

Several inhibitors of thyroid iodide uptake activity were identified before the molecular identity of NIS was revealed. These include two sodium competitors [46] and several chloride channel blockers [47]. Molecules such as dysidenin, 5-(N,N-hexamethylene)amiloride (HMA) and econazole also induce reversible, noncompetitive or mixed inhibition of iodide transport [48]. More recently, aryltrifluoroborates were shown to inhibit NIS function [49] and a library of 17,020 chemical compounds was tested using a high-throughput screening method [50,51] with transfected, cultured mammalian cells. Amongst the identified molecules [51], ten were studied in more detail using the *Xenopus* oocyte expression system. These studies revealed a high diversity in the mode of action of the different molecules [52]. The chemical structures of the four most powerful inhibitors (>90% inhibition) tested in this study are shown in Fig. 2. A structure–activity relationship study was performed on 115 derivatives of one of these inhibitors (3,4-dihydropyrimidin-2(1H)-ones) [53] and on the racemates of three dihydropyrimidin-2-ones, showing that most of the inhibitory activity is a feature of one enantiomer [54]. These molecules represent putative tools for further functional (and structural) characterization of NIS at the molecular level.

5. NIS orthologs

Interestingly, functional differences have been identified between mouse or rat NIS (mNIS or rNIS, respectively) and human NIS (hNIS). The rat and the mouse orthologs were shown to accumulate radioisotopes more efficiently than the human protein [43,55]. The molecular basis of these functional differences could be helpful for further characterization of NIS. Zhang and collaborators showed that rNIS is localized in a higher proportion at the plasma membrane than hNIS and the N-terminal region up to putative TM7 appears to be involved in this difference [56]. These authors also reported differences in the kinetics of the Na^+ binding, implicating the region spanning from TM4 to TM6 and Ser200 of hNIS. They, thus, proposed that this region could be involved in sodium binding [56]. In our laboratory, it was shown that the V_{max} of the mouse protein is four times higher than the V_{max} of the human protein when expressed in the same cell line (HEK-293) [43] (Fig. 3, panel C). The K_{mI} value determined for hNIS (9.0 ± 0.8 μM) was significantly lower than the K_{mI} for the mouse protein (26.4 ± 3.5 μM) whereas the K_{mNa} values were not significantly different. Similarly to the rat protein, mNIS is predominantly localized in the plasma membrane whereas the human ortholog is detected intracellularly in 40% of the cells in which it is expressed (Fig. 3, panels A and B). However, the difference in the V_{max} values does not only seem to be related to the higher intracellular localization of hNIS. Using chimeric proteins between human and mouse NIS, we showed that the N-terminal region up to TM8 is most probably involved in iodide binding, and that the region from TM5 to the C terminus could play an important role in targeting the protein to the plasma membrane [43]. One of the long-term goals of these studies is the engineering of a chimeric NIS protein most suitable for gene therapy, i.e. preserving regions responsible for the high turnover rate and the efficient plasma membrane localization of the mouse protein while replacing the immunogenic extracellular regions with those of the human ortholog.

The porcine NIS gene gives rise to splice variants leading to three active NIS proteins with differences in their C-terminal extremities [4]. However, it is not known if these differences lead to distinct properties.

6. NIS family

NIS belongs to the sodium/solute symporter family (SSSF) in the transporter classification system [57] and to the SLC5 family in the solute carrier nomenclature [58,59]. Most of the members of these families are symporters and mediate the uptake of a variety of molecules: sugars, amino acids, monocarboxylates, myo-inositol, vitamins (pantothenate, biotin), urea and anions (iodide, thiocyanate, perchlorate) [6,60,61]. Others are substrate-activated channels, such as human SGLT3 (SLC5A4) [61,62]. Fig. 4 represents a sequence alignment of some SLC5 members with vSGLT. The sodium/solute transporters are widely encountered in bacteria, Archaea, plants and animals. Concerning solute selectivity, it has been reported recently that SLC5A6 (SMVT, multivitamin transporter) transports iodide [63] and that several members of the family, including NIS and the sodium/glucose symporter isoform 1 (SGLT1), are able to transport urea and water (cotransport or channel) [32,64–67]. In this family, as for many other symporters, the inward Na^+ gradient and the negative membrane potential drive the transport of the substrates into the cells and several members also behave as uniporters [29,67,68].

The transport stoichiometry varies between different transporters and can also differ for the same protein depending on the substrate transported. For example, a sodium-dependent, 2:1 transport stoichiometry has been described for NIS (iodide), SGLT1 (glucose) and SMVT (vitamin), whereas a 1:1 ratio was detected for PutP (proline) and vSGLT (galactose) [6,69]. For NIS, the ratio is 2:1 for iodide as mentioned above, but 1:1 with perchlorate [31].

Members of the SSS family vary greatly in size, being composed of between 500 and 700 amino acid residues [6,60,61]. They contain between

thirteen and fifteen predicted transmembrane helices. In 2008, Faham and collaborators reported the 3D structure (about 3.0 Å resolution) of the *Vibrio parahaemolyticus* sodium/galactose symporter (vSGLT) [37]. The structure clearly showed fourteen transmembrane helices with extracellular amino and carboxy termini. A structural feature of this transporter is an inverted repeat of five transmembrane helices (i.e. TM2 to TM6 and TM7 to TM11), which is probably also encountered in other sodium symporters [70] such as NIS. The structure was obtained in the presence of sodium and galactose in an inward-facing, occluded conformation with one galactose molecule bound in the centre of the protein [37]. It was, therefore, possible to determine all the residues contributing to the galactose binding site in this conformation and the residues forming the gates. These residues are not well conserved in NIS. In contrast, the amino acid residues involved in Na^+ binding are found in equivalent positions in vSGLT and in NIS. In 2010, Watanabe et al. published another structure of vSGLT in the inward-open conformation. They performed a comprehensive study, including molecular dynamic simulations, to better understand the mechanisms of cotransport and sodium and substrate binding and release [38].

Several biophysical and biochemical experiments (including AFM, mass spectrometry, spin labeling and cysteine accessibility), coupled with mutagenesis, have been performed to study the sodium/proline or sodium/glucose symporters and their conformational changes upon substrate binding [38,71–73]. Amongst the data obtained, we can note that, in the sodium/proline symporter, TM2 contributes to the cation and proline binding sites [74,75]. TM9 is also essential in PutP and studies suggest that it contributes to the formation of a hydrophilic cavity and probably to the sodium and/or proline translocation pathway [76]. Regarding the high-affinity sodium/glucose cotransporter, it has been shown that TM4 participates in sugar binding [77] and that the C-terminal loop 13 is implicated in substrate recognition [78]. Taken together, these results are probably transposable to other members of the family, including NIS.

7. NIS structure/function relationship

To date, knowledge of the NIS structure/function relationship has been mainly obtained from studies of NIS gene mutations leading to congenital iodine transport defects (ITD). These mutations are shown on an amino acid sequence alignment of NIS with vSGLT (Fig. 4) and on a 3D structure model using vSGLT as a template [37,38] (Fig. 5). Their effects are also summarized in a table in the supplementary data (Table S1). Fourteen NIS mutations have been identified in ITD to date and twelve of these are described in the review of Spitzweg and Morris [79]. They lead to either the synthesis of truncated proteins [80,81], proteins with partial deletions [82–85] or amino acid substitutions [81,86–90]. Some have been further characterized at the molecular level. The V59E mutation is located close to the cytosolic side of putative TM2 (corresponding toTM2I in the vSGLT structure, see Fig. 4) and causes a complete loss of NIS function [91]. Charged amino acid residues, or a proline residue at position 59, directly affect the protein function, while replacements with neutral, helix-promoting residues are well tolerated. No effects on I^- or Na^+ K_m values were observed. These results, together with the particular localization of the mutation, suggest a role of V59 in helix–helix interactions during the transport cycle. Based on the ITD associated with the G93R mutation, Paroder-Belenitsky and collaborators [92] studied this particular position in putative TM3 in more detail. They found that lengthening the neutral side chain increases the K_m for the transported anions. More strikingly, changing the glycine residue to threonine, asparagine, glutamine, or an acidic residue, alters the stoichiometry of perchlorate transport, which is no longer electro neutral. The selectivity for the different anions is also modified in G93E and G93Q variants. To interpret these findings, the authors performed a basic homology modeling of NIS using the vSGLT structure as a template. They concluded that G93 and Trp255, an amino acid residue in close contact, form a "ball-and-socket joint" implicated in the control of the inward/outward conformational changes as well as in the stoichiometry [92]. The R124H mutation was described by Szinnai and collaborators [90]. This residue is located in intracellular helix 3 (IL3). The mutation abolishes NIS iodide uptake activity in cells, but, according to these authors, does not impair targeting. More recently, Paroder and collaborators [93] showed that, to the contrary, R124H NIS protein localizes in the ER and is incompletely glycosylated, but is functional in membrane vesicles. They also studied other mutations at this position and concluded that a δ amino group is critical for proper maturation and membrane trafficking of the protein [93]. They propose an interaction of R124 with C440, which could be important for local folding of NIS. One can note that an arginine residue at an equivalent position is conserved in vSGLT. F177L (published as F176L) and A180T mutations also caused a moderate decrease in iodide accumulation even though the protein was expressed at a normal level and properly targeted [56]. Zhang and collaborators [56] analysed the causes of the differences in transport activity observed between rat and human NIS. They found a difference in the kinetics of Na^+ binding between the two orthologs and proposed that S200 of hNIS plays a role in Na^+ binding. It should be mentioned that no equivalent position has been identified as an Na^+ site on the crystal structure of vSGLT and, thus, the effect may be indirect (due to a conformational change). de la Vieja and collaborators [5,94] demonstrated that Q267E NIS is properly addressed to the plasma membrane but has a very low catalytic turnover rate. A glutamine residue at an equivalent position is conserved in vSGLT. This residue is located in TM7I, which is part of the inverted repeat [37]. Substitution of Q267 by other charged residues always leads to an inactive transporter, while neutral amino acids (such as Asn or Ala) lead to a protein with partial transport activity (30% and 20% of WT NIS activity, respectively). The deletion of two amino acid residues (287 and 288) described by Montanelli and collaborators [85] leads to a complete absence of iodide uptake and is, according to the sequence alignment (see Fig. 4), located in TM8 next to an amino acid residue implicated in glucose binding in the vSGLT structure. This region is thus probably also important in NIS for substrate binding/translocation. Analysis of the T354P mutation [95] revealed the importance at this position of the hydroxyl group on the threonine beta-carbon for NIS function and led to the finding that other hydroxyl-containing residues surrounding T354 in TM9 are also required for NIS function [96]. For mutant NIS at these positions, higher K_m values were found for Na^+ than WT NIS, suggesting that TM9 may be involved in Na^+ binding and/or translocation. Interestingly, the equivalent position of T354 in the crystal structure of vSGLT [37], i.e. S365 (see Fig. 4), has been identified as part of the Na^+ binding site. Similarly to the Q267E mutation, the G395R mutation in putative TM10 disrupts NIS function but not its expression and targeting [97]. The presence of an uncharged amino acid with a small side chain at this position is essential for NIS function. The finding that active constructs show a lower turnover (V_{max}) but

Fig. 4. NIS family. This figure represents a multiple sequence alignment of sodium/solute family members performed with ClustalW2 [120] and refined manually. The sequences of vSGLT, SGLT1 (SLC5A1), SGLT3 (SLC5A4), NIS (SLC5A5), SMVT (SLC5A6) and PutP from *Escherichia coli* are shown up to the twelfth transmembrane helix, as this represents the most conserved region. Residue letters are colored according to their nature (red, small+hydrophobic including aromatic residues except Y: AVFPMILW; blue, acidic D, E; magenta, basic, R, K; green, hydroxyl+sulfhydryl+amide+G, STYCHNQG). Strictly, highly and weakly conserved residues (as defined in ClustalW) are highlighted in black, gray or light-gray boxes, respectively. The transmembrane helices of vSGLT are shown above as well as residues involved in transport function, as defined by Faham et al. [37]: gray — hydrophobic plug residues; blue — substrate binding residues; yellow — sodium-binding residue. NIS mutations important for transport function, and described in the NIS structure/function relationship section, are shown below the sequences. They are designated as squares, leading to: green — transport defect (V59 [89,91], G93 [87,92], R124 [90,93], Q267 [81,94,121], Delta287–288 [85], G395 [88,97], N441 [98] and all the charged residues E79, R82, K86, D163, H226, R228, D233, D237, R239, R241, D311, D322, D331 [100,101]); and yellow — sodium-binding defect (S200 [56], T351, S353, T354, S356, T357 and N360 [86,87,96]).

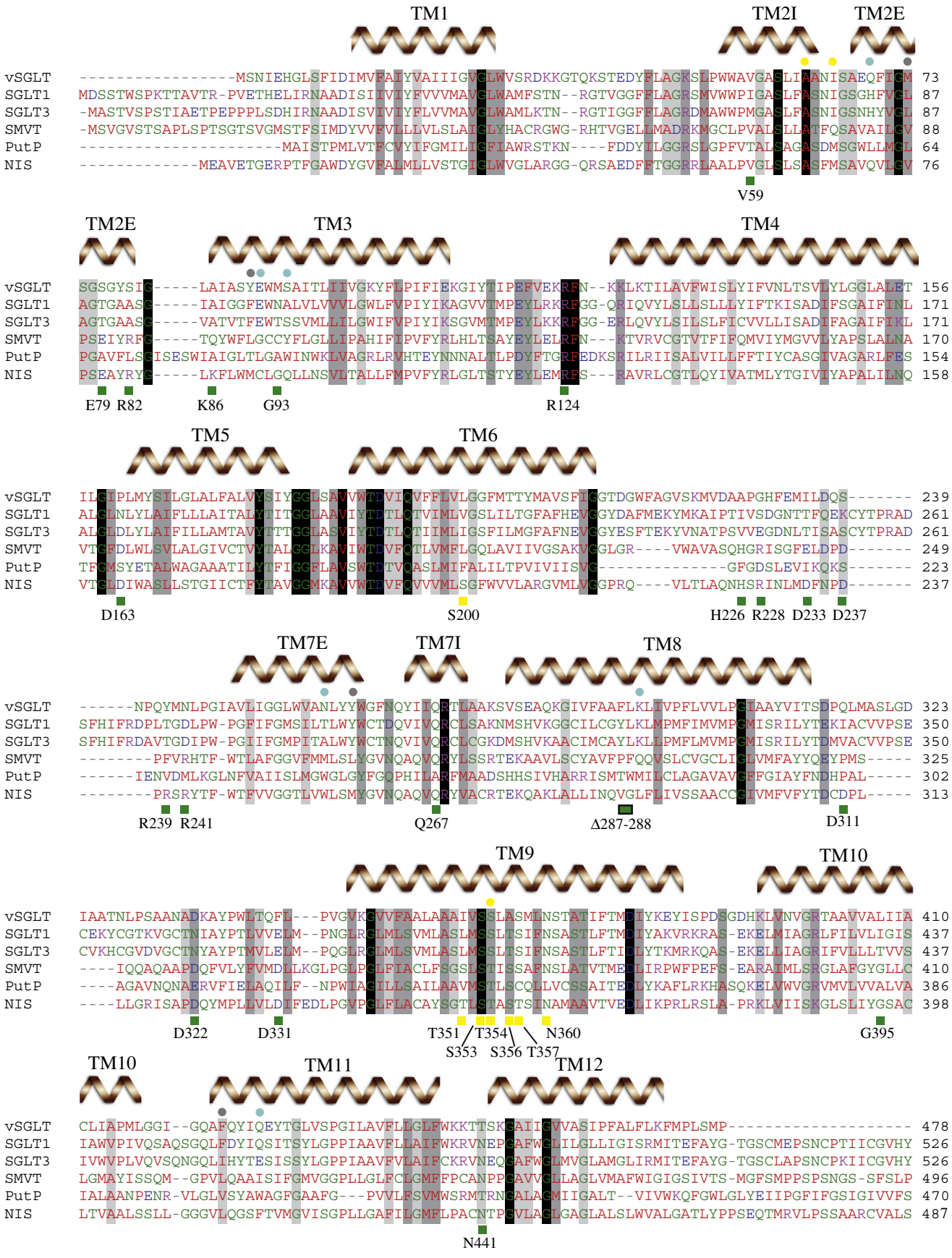
TM1
TM2I
TM2E
vSGLT ----------MSNIEHGLSFIDIMVFAIYVAIIIGVGLWVSRDKKGTQKSTEDYFLAGKSLPWWAVGASLIAANISAEQFIGM 73
SGLT1 MDSSTWSPKTTAVTR-PVETHELIRNAADISIIVIYFVVVMAVGLWAMFSTN--RGTVGGFFLAGRSMVWWPIGASLFASNIGSGHFVGL 87
SGLT3 -MASTVSPSTIAETPEPPPLSDHIRNAADISVIVIYFLVVMAVGLWAMLKTN--RGTIGGFFLAGRDMAWWPMGASLFASNIGSNHYVGL 87
SMVT -MSVGVSTSAPLSPTSGTSVGMSTFSIMDYVVFVLLLVLSLAIGLYHACRGWG-RHTVGELLMADRKMGCLPVALSLLATFQSAVAILGV 88
PutP ----------MAISTPMLVTFCVYIFGMILIGFIAWRSTKN----FDDYILGGRSLGPFVTALSAGASDMSGWLLMGL 64
NIS ----------MEAVETGERPTFGAWDYGVFALMLLVSTGIGLWVGLARGG-QRSAEDFFTGGRRLAALPVGLSLSASFMSAVQVLGV 76
V59
TM2E
TM3
TM4
vSGLT SGSGYSIG-----LAIASYEWMSAITLIIVGKYFLPIFIEKGIYTIPEFVEKRFN--KKLKTILAVFWISLYIFVNLTSVLYLGGLALET 156
SGLT1 AGTGAASG-----IAIGGFEWNALVLVVVLGWLFVPIYIKAGVVTMPEYLRKRFGG-QRIQVYLSLLSLLLYIFTKISADIFSGAIFINL 171
SGLT3 AGTGAASG-----VATVTFEWTSSVMLLILGWIFVPIYIKSGVMTMPEYLKKRFGG-ERLQVYLSILSLFICVVLLISADIFAGAIFIKL 171
SMVT PSEIYRFG-----TQYWFLGCCYFLGLLIPAHIFIPVFYRLHLTSAYEYLELRFN---KTVRVCGTVTFIFQMVIYMGVVLYAPSLALNA 170
PutP PGAVFLSGISESWIAIGLTLGAWINWKLVAGRLRVHTEYNNNALILPDYFTGRFEDKSRILRIISALVILLFFTIYCASGIVAGARLFES 154
NIS PSEAYRYG-----LKFLWMCLGQLLNSVLTALLFMPVFYRLGLTSTYEYLEMRFS---RAVRLCGTLQYIVATMLYTGIVIYAPALILNQ 158
E79 R82 K86 G93 R124
TM5
TM6
vSGLT ILGIPLMYSILGLALFALVYSIYGGLSAVVWTDVIQVFFLVLGGFMTTYMAVSFLGGTDGWFAGVSKMVDAAPGHFEMILDQS------- 239
SGLT1 ALGLNLYLAIFLLLAITALYTITGGLAAVIYTDTLQTVIMLVGSLILTGFAFHEVGGYDAFMEKYMKAIPTIVSDGNTTFQEKCYTPRAD 261
SGLT3 ALGLDLYLAIFILLAMTAVYTTTGGLASVIYTDTLQTIIMLIGSFILMGFAFNEVGGYESFTEKYVNATPSVVEGDNLTISASCYTPRAD 261
SMVT VTGFDLWLSVLALGIVCTVYTALGGLKAVIWTDVFQTLVMFLGGLAVIIVGSAKVGGLGR----VWAVASQHGRISGFELDPD------- 249
PutP TFGMSYETALWAGAAATILYTFIGGFLAVSWTDTVQASLMIFALILTPVIVIISVG--------------GFGDSLEVIKQKS------- 223
NIS VTGLDIWASLLSTGIICTFYTAVGGMKAVVWTDVFQVVVMLSGFWVVLARGVMLVGGPRQ----VLTLAQNHSRINLMDFNPD------- 237
D163 S200 H226 R228 D233 D237
TM7E
TM7I
TM8
vSGLT ------NPQYMNLPGIAVLIGGLWVANLYYWGFNQYIIQRTLAAKSVSEAQKGIVFAAFLKLIVPFLVVLPGIAAYVITSDPQLMASLGD 323
SGLT1 SFHIFRDPLTGDLPW-PGFIFGMSILTLWYWCTDQVIVQRCLSAKNMSHVKGGCILCGYLKLLPMFIMVMPGMISRILYTEKIACVVPSE 350
SGLT3 SFHIFRDAVTGDIPW-PGIIFGMPITALWYWCTNQVIVQRCLCGKDMSHVKAACIMCAYLKLLPMFLMVMPGMISRILYTDMVACVVPSE 350
SMVT --------PFVRHTF-WTLAFGGVFMMLSLYGVNQAQVQRYLSSRTEKAAVLSCYAVFPFQQVSLCVGCLIGLVMFAYYQEYPMS----- 325
PutP ------IENVDMLKGLNFVAIISLMGWGLGYFGQPHILARFMAADSHHSIVHARRISMTWMILCLAGAVAVGFFGIAYFNDHPAL----- 302
NIS --------PRSRYTF-WTFVVGGTLVWLSMYGVNQAQVQRYVACRTEKQAKLALLINQVGLFLIVSSAACCGIVMFVFYTDCDPL----- 313
R239 R241 Q267 Δ287-288 D311
TM9
TM10
vSGLT IAATNLPSAANADKAYPWLTQFL---PVGVKGVVFAALAAAIVSSLASMLNSTATIFTMDIYKEYISPDSGDHKLVNVGRTAAVVALIIA 410
SGLT1 CEKYCGTKVGCTNIAYPTLVVELM--PNGLRGLMLSVMLASLMSSLISIFNSASTLFTMDIYAKVRKRAS-EKELMIAGRLFILVLIGIS 437
SGLT3 CVKHCGVDVGCTNYAYPTMVLELM--PQGLRGLMLSVMLASLMSSLTSIFNSASTLFTIDLYTKMRKQAS-EKELLIAGRIFVLLLTVVS 437
SMVT ----IQQAQAAPDQFVLYFVMDLLKGLPGLPGLFIACLFSGSLSTISSAFNSLATVTMEDLIRPWFPEFS-EARAIMLSRGLAFGYGLLC 410
PutP ----AGAVNQNAERVFIELAQILF--NPWIAGLLLSAILAAVMSTLSCQLLVCSSAITEDLYKAFLRKHASQKELVWVGRVMVLVVALVA 386
NIS ----LLGRISAPDQYMPLLVLDIFEDLPGVPGLFLACAYSGTLSTASTSINAMAAVTVEDLIKPRLRSLA-PRKLVIISKGLSLIYGSAC 398
D322 D331 T351 T354 N360 G395
S353 S356 T357
TM10
TM11
TM12
vSGLT CLIAPMLGGI--GQAFQYIQEYTGLVSPGILAVFLLGLFWKKTTSKGAIIGVVASIPFALFLKFMPLSMP------------------- 478
SGLT1 IAWVPIVQSAQSGQLFDYIQSITSYLGPPIAAVFLLAIFWKRVNEPGAFWGLILGLLIGISRMITEFAYG-TGSCMEPSNCPTIICGVHY 526
SGLT3 IVWVPLVQVSQNGQLIHYTESISSYLGPPIAAVFVLAIFCKRVNEQGAFWGLMVGLAMGLIRMITEFAYG-TGSCLAPSNCPKIICGVHY 526
SMVT LGMAYISSQM--GPVLQAAISIFGMVGGPLLGLFCLGMFFPCANPPGAVVGLLAGLVMAFWIGIGSIVTS-MGFSMPPSPSNGS-SFSLP 496
PutP IALAANPENR-VLGLVSYAWAGFGAAFG---PVVLFSVMWSRMTRNGALAGMIIGALT--VIVWKQFGWLGLYEIIPGFIFGSIGIVVFS 470
NIS LTVAALSSLL-GGGVLQGSFTVMGVISGPLLGAFILGMFLPACNTPGVLAGLGAGLALSLWVALGATLYPPSEQTMRVLPSSAARCVALS 487
N441

similar affinities for I^- and Na^+ (K_m) than wild type NIS, led the authors to speculate that only a small amino acid at position 395 allows for the rotation of TM10 during the transport process. In vSGLT, TM10 is not part of the central helices responsible for binding galactose. Based on the data that the deletion variant Delta439–443 leads to ITD [83], Li and collaborators [98] studied this region. Their main finding is that N441 is critical for proper folding and function of the symporter, by capping the α-helix of TM12. This highlights the structural importance of the interhelical interaction in this region. An asparagine residue at an equivalent position is conserved in almost all SLC5 family members. In vSGLT, a threonine residue performs the capping function. In contrast with the other mutants (except R124H), de la Vieja and collaborators showed that the G543E mutation (cytosolic end of TM13) is responsible for a maturation defect and improper targeting of the protein to the plasma membrane [99]. Small, neutral amino acids rescued some iodide uptake, suggesting that a tightly packed area is required in this domain.

Wu and collaborators [100] identified amongst several NIS homologues a conserved histidine residue (H226) in extracellular loop 4 (EL4). Replacement of H226 by an Ala, Asp, Glu or Lys residue leads to a complete loss of transport activity. Therefore, Li and collaborators studied the substitution by alanine of fourteen conserved charged amino acids in the extracellular NIS segments [101]. Apart from Arg 9, all of the thirteen remaining mutations severely impaired NIS function. Mutations at positively charged residues decreased V_{max}, while most of the mutations at negatively charged residues increased the K_m for I^- with respect to WT NIS.

Despite these numerous studies using NIS variants, mainly in the context of thyroid pathology, the understanding of the roles of residues is still limited and will benefit greatly from molecular modeling.

8. Post-translational regulation of NIS

NIS is a protein that is finely regulated at the transcriptional level, including epigenetic regulation [8,102], and at the post-translational level, especially in relation to its subcellular localization. In the thyroid, the protein is located at the basolateral membrane of the follicular cells, whereas for some tissues an apical localization has been described [25,26] suggesting that the NIS membrane targeting in polarized cells is cell-type dependent. Under physiological conditions, TSH and iodide control the protein expression level and its localization to the thyroid plasma membrane (promoted by TSH [33,103,104] and inhibited by an excess of iodide [105,106]). In a majority of tumors from the thyroid, breast and other tissues, intracellular NIS expression has been observed by immunocytochemistry [22,107,108]. More recently, Peyrottes et al. demonstrated, using a set of monoclonal antibodies and western blot analyses, that NIS expression is in fact low in various human thyroid and breast cancers [42] and that the intracellular staining corresponds to nonspecific signal. This inappropriate staining may therefore lead researchers to focus on NIS translocation (post-translational regulation) in order to increase iodide uptake for radiotherapy, whereas they should in fact first study its transcriptional and epigenetic regulation. It can also be noted that increasing NIS mRNA does not necessarily increase iodide uptake activity, as exemplified by the PI3KCA-selective inhibitor, PI-103 [109]. Knostman and collaborators showed that PI3K activation in a human mammary carcinoma cell line (MCF-7) increases expression of under-glycosylated NIS and impairs trafficking to the plasma membrane [110]. In 2007, Vadysirisack et al. [111] revealed that MEK signaling affects NIS regulation in thyroid cells. More recently, Zhang et al. showed that MEK inhibition leads to NIS lysosomal degradation in human breast cancer cells [112]. The MEK signaling pathway is important in oncogenic transformation and appears to be a key element in NIS protein stability, at least in breast cancers. Very few data are, however, yet available regarding these processes at the molecular level.

Many potential regulation sites that are subject to post-translational modification (phosphorylation, sumoylation, ubiquitinylation), or sites of protein/protein interaction (SH3 or SH2 binding motifs, tyrosine-based motifs, PDZ domain protein binding sites…), are predicted by bioinformatics to be present on this protein, mainly at the C-terminal domain.

A first study by Vadysirisack et al. focused on NIS phosphorylation [36]. These authors identified five in vivo phosphorylation sites in rat NIS: the phosphorylation status of S227, which is predicted to be extracellular, is functionally silent, whereas that of S43 and S581 modulates iodide transport velocity, and that of T577 modulates NIS stability. The T49 residue seems to be important for protein stability. Marsee et al., in 2004, proposed that hsp90 may function as a chaperone for NIS folding, as it does for a limited number of other integral membrane proteins [113]. In 2009, Smith et al. showed that PTTG binding factor (a proto-oncogene implicated in thyroid cancers) binds to NIS and promotes its intracellular retention [114]. More recently, a study based on a yeast two-hybrid system unveiled the interaction of NIS with the Rho-guanine nucleotide-exchange factor, LARG, and its role in the regulation of cancer cell motility and invasiveness [115]. This interaction is mediated by the PDZ binding site at the C-terminal extremity of NIS and the PDZ domain of LARG, however in this case it seems that NIS acts, rather, as a regulator by preventing the interaction of LARG with the small GTPase, RhoA. Other studies based on PDZ arrays (manuscript in preparation) indicate that several proteins containing PDZ domains modulate NIS targeting. However, more work is clearly needed to obtain a full picture of all of these interactions.

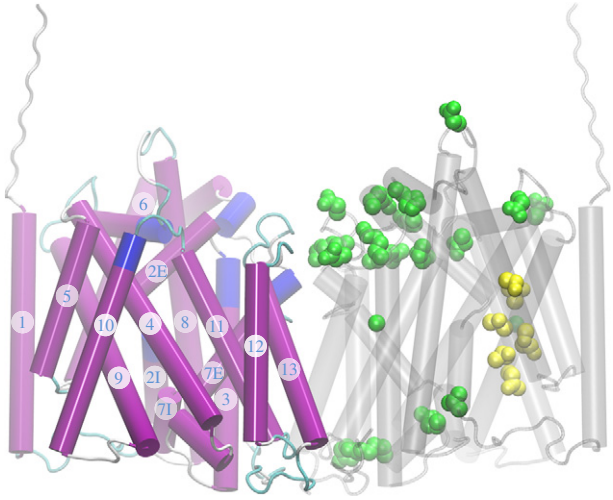

Fig. 5. NIS 3D homology model. A preliminary NIS model was built using the protein template of vSGLT (PDB ID: 2XQ2, [38]) with an in-house, semi-automated protocol [122]. Several missing residues in vSGLT template (PDB ID: 2XQ2) were replaced by the corresponding ones present in the WT structure of vSGLT (PDB ID: 3DH4 [37]). The initial sequence alignment between vSGLT and NIS was performed using ClustalW2 [120] and fully refined using INTERALIGN [123]. The current model includes residues 1 to 562, except the very long extracellular loop (468–520). Cartesian coordinates of all atoms were energy-minimized as previously described [124] and the dimeric structure was built by superimposing the NIS model on the dimer crystal structure of vSGLT template (PDB ID: 2XQ2 using Sup3d [122]. The image was created and rendered using VMD [125]. The structure of one monomer is shown in purple (alpha helices), blue (3–10 helices), cyan (turns), and white (coils). TM helices are labeled with white dots. The other monomer is shown in transparency and the different NIS mutations defined in Fig. 4 are highlighted in spacefill representation (green — transport defect; yellow — sodium-binding defect).

9. NIS molecular characterization in the future

Little is currently known about the structure of NIS. A first attempt to investigate this included homology modeling of NIS with the glycerol-3-phosphate transporter [100] and, more recently, vSGLT structures PDB ID: 3DH4 [92] or PDB ID: 2XQ2 (our laboratory, Fig. 5) as templates. However, careful molecular modeling will be essential to fully exploit the crystallographic data. In particular, molecular dynamic simulations will be required with the protein inserted in a lipid bilayer, and taking

into account a probable dimeric assembly of the transporter. The discovery that the structural core of inverted repeats is common with other sodium symporters (LeuT, Mhp1 and betP) of different families, and the fact that they are crystallized in different conformations during the transport cycle, will add invaluable mechanistic information [70]. The different proteins are not well conserved outside of their core and it is known that some of these regions are nonetheless essential for protein function. For example, loop 13 of SGLT is involved in substrate recognition [78] but no homologous part can be found in NIS. This region of NIS corresponding to its C-terminal domain will therefore necessitate ab initio modeling. In all cases, these homology models will allow a more targeted mutagenesis of the protein and contribute to a full understanding of the NIS structure/function relationship and transport mechanism.

Another major challenge concerning the molecular characterization of NIS is to understand the underlying mechanisms of the post-translational regulation of the protein. Thorough analyses are required to elucidate the implication of the different amino acid residues and predicted sites in protein/protein interactions, targeting and transporter stability. It will also be necessary to explore the role of dimerization and the potential implication of the C-terminal fragment in NIS function and regulation [44]. Finally, although a small number of interacting partners have already been pinpointed ([114,115] and manuscript in preparation), many still need to be identified in order to understand the regulation of this essential protein at the molecular level.

Supplementary data to this article can be found online at http://dx.doi.org/10.1016/j.bbamem.2013.08.013.

Acknowledgements

We would like to thank Patrick Chang for a careful reading of the manuscript.

References

[1] G. Dai, O. Levy, N. Carrasco, Cloning and characterization of the thyroid iodide transporter, Nature 379 (1996) 458–460.
[2] P.A. Smanik, Q. Liu, T.L. Furminger, K. Ryu, S. Xing, E.L. Mazzaferri, S.M. Jhiang, Cloning of the human sodium iodide symporter, Biochem. Biophys. Res. Commun. 226 (1996) 339–345.
[3] B. Perron, A.M. Rodriguez, G. Leblanc, T. Pourcher, Cloning of the mouse sodium iodide symporter and its expression in the mammary gland and other tissues, J. Endocrinol. 170 (2001) 185–196.
[4] S. Selmi-Ruby, C. Watrin, S. Trouttet-Masson, F. Bernier-Valentin, V. Flachon, Y. Munari-Silem, B. Rousset, The porcine sodium/iodide symporter gene exhibits an uncommon expression pattern related to the use of alternative splice sites not present in the human or murine species, Endocrinology 144 (2003) 1074–1085.
[5] A. De La Vieja, O. Dohan, O. Levy, N. Carrasco, Molecular analysis of the sodium/iodide symporter: impact on thyroid and extrathyroid pathophysiology, Physiol. Rev. 80 (2000) 1083–1105.
[6] H. Jung, The sodium/substrate symporter family: structural and functional features, FEBS Lett. 529 (2002) 73–77.
[7] O. Dohan, A. De la Vieja, V. Paroder, C. Riedel, M. Artani, M. Reed, C.S. Ginter, N. Carrasco, The sodium/iodide Symporter (NIS): characterization, regulation, and medical significance, Endocr. Rev. 24 (2003) 48–77.
[8] T. Kogai, G.A. Brent, The sodium iodide symporter (NIS): regulation and approaches to targeting for cancer therapeutics, Pharmacol. Ther. 135 (2012) 355–370.
[9] G. Riesco-Eizaguirre, P. Santisteban, A perspective view of sodium iodide symporter research and its clinical implications, Eur. J. Endocrinol. 155 (2006) 495–512.
[10] M. Schlumberger, L. Lacroix, D. Russo, S. Filetti, J.M. Bidart, Defects in iodide metabolism in thyroid cancer and implications for the follow-up and treatment of patients, Nat. Clin. Pract. Endocrinol. Metab. 3 (2007) 260–269.
[11] D.P. Carvalho, A.C. Ferreira, The importance of sodium/iodide symporter (NIS) for thyroid cancer management, Arq. Bras. Endocrinol. Metabol. 51 (2007) 672–682.
[12] M. Hingorani, C. Spitzweg, G. Vassaux, K. Newbold, A. Melcher, H. Pandha, R. Vile, K. Harrington, The biology of the sodium iodide symporter and its potential for targeted gene delivery, Curr. Cancer Drug Targets 10 (2010) 242–267.
[13] A.L. Ho, R.K. Grewal, R. Leboeuf, E.J. Sherman, D.G. Pfister, D. Deandreis, K.S. Pentlow, P.B. Zanzonico, S. Haque, S. Gavane, R.A. Ghossein, J.C. Ricarte-Filho, J.M. Dominguez, R. Shen, R.M. Tuttle, S.M. Larson, J.A. Fagin, Selumetinib-enhanced radioiodine uptake in advanced thyroid cancer, N. Engl. J. Med. 368 (2013) 623–632.
[14] M. Dayem, V. Navarro, R. Marsault, J. Darcourt, S. Lindenthal, T. Pourcher, From the molecular characterization of iodide transporters to the prevention of radioactive iodide exposure, Biochimie 88 (2006) 1793–1806.
[15] C. Spitzweg, J.C. Morris, The sodium iodide symporter: its pathophysiological and therapeutic implications, Clin. Endocrinol. (Oxf) 57 (2002) 559–574.
[16] J. Faivre, J. Clerc, R. Gerolami, J. Herve, M. Longuet, B. Liu, J. Roux, F. Moal, M. Perricaudet, C. Brechot, Long-term radioiodine retention and regression of liver cancer after sodium iodide symporter gene transfer in wistar rats, Cancer Res. 64 (2004) 8045–8051.
[17] G. Riesco-Eizaguirre, A. De la Vieja, I. Rodriguez, S. Miranda, P. Martin-Duque, G. Vassaux, P. Santisteban, Telomerase-driven expression of the sodium iodide symporter (NIS) for in vivo radioiodide treatment of cancer: a new broad-spectrum NIS-mediated antitumor approach, J. Clin. Endocrinol. Metab. 96 (2011) E1435–E1443.
[18] W. Li, J. Tan, P. Wang, N. Li, F. Zhang, The glial fibrillary acidic protein promoter directs sodium/iodide symporter gene expression for radioiodine therapy of malignant glioma, Oncol. Lett. 5 (2013) 669–674.
[19] K. Knoop, N. Schwenk, P. Dolp, M.J. Willhauck, C. Zischek, C. Zach, M. Hacker, B. Goke, E. Wagner, P.J. Nelson, C. Spitzweg, Stromal targeting of sodium iodide symporter using mesenchymal stem cells allows enhanced imaging and therapy of hepatocellular carcinoma, Hum. Gene Ther. 24 (2013) 306–316.
[20] S.M. Jhiang, J.Y. Cho, K.Y. Ryu, B.R. DeYoung, P.A. Smanik, V.R. McGaughy, A.H. Fischer, E.L. Mazzaferri, An immunohistochemical study of Na^+/I^- symporter in human thyroid tissues and salivary gland tissues, Endocrinology 139 (1998) 4416–4419.
[21] K.M. La Perle, D.C. Kim, N.C. Hall, A. Bobbey, D.H. Shen, R. Nagy, P.E. Wakely Jr., A. Lehman, D. Jarjoura, S.M. Jhiang, Modulation of sodium/iodide symporter expression in the salivary gland, Thyroid (2013), http://dx.doi.org/10.1089/thy.2012.0571.
[22] U.H. Tazebay, I.L. Wapnir, O. Levy, O. Dohan, L.S. Zuckier, Q. Hua Zhao, H. Fu Deng, P.S. Amenta, S. Fineberg, R.G. Pestell, N. Carrasco, The mammary gland iodide transporter is expressed during lactation and in breast cancer, Nat. Med. 6 (2000) 871–878.
[23] J.Y. Cho, R. Leveille, R. Kao, B. Rousset, A.F. Parlow, W.E. Burak Jr., E.L. Mazzaferri, S.M. Jhiang, Hormonal regulation of radioiodide uptake activity and Na^+/I^- symporter expression in mammary glands, J. Clin. Endocrinol. Metab. 85 (2000) 2936–2943.
[24] M.A. Fragoso, V. Fernandez, R. Forteza, S.H. Randell, M. Salathe, G.E. Conner, Transcellular thiocyanate transport by human airway epithelia, J. Physiol. 561 (2004) 183–194.
[25] J.P. Nicola, C. Basquin, C. Portulano, A. Reyna-Neyra, M. Paroder, N. Carrasco, The Na^+/I^- symporter mediates active iodide uptake in the intestine, Am. J. Physiol. Cell Physiol. 296 (2009) C654–C662.
[26] T. Kotani, Y. Ogata, I. Yamamoto, Y. Aratake, J.I. Kawano, T. Suganuma, S. Ohtaki, Characterization of gastric Na^+/I^- symporter of the rat, Clin. Immunol. Immunopathol. 89 (1998) 271–278.
[27] J.M. Bidart, L. Lacroix, D. Evain-Brion, B. Caillou, V. Lazar, R. Frydman, D. Bellet, S. Filetti, M. Schlumberger, Expression of Na^+/I^- symporter and Pendred syndrome genes in trophoblast cells, J. Clin. Endocrinol. Metab. 85 (2000) 4367–4372.
[28] D. Russo, A. Scipioni, C. Durante, E. Ferretti, L. Gandini, V. Maggisano, D. Paoli, A. Verrienti, G. Costante, A. Lenzi, S. Filetti, Expression and localization of the sodium/iodide symporter (NIS) in testicular cells, Endocrine 40 (2011) 35–40.
[29] S. Eskandari, D.D. Loo, G. Dai, O. Levy, E.M. Wright, N. Carrasco, Thyroid Na^+/I^- symporter. Mechanism, stoichiometry, and specificity, J. Biol. Chem. 272 (1997) 27230–27238.
[30] J. Van Sande, C. Massart, R. Beauwens, A. Schoutens, S. Costagliola, J.E. Dumont, J. Wolff, Anion selectivity by the sodium iodide symporter, Endocrinology 144 (2003) 247–252.
[31] O. Dohan, C. Portulano, C. Basquin, A. Reyna-Neyra, L.M. Amzel, N. Carrasco, The Na^+/I symporter (NIS) mediates electroneutral active transport of the environmental pollutant perchlorate, Proc. Natl. Acad. Sci. U. S. A. 104 (2007) 20250–20255.
[32] T. Zeuthen, B. Belhage, E. Zeuthen, Water transport by Na^+-coupled cotransporters of glucose (SGLT1) and of iodide (NIS). The dependence of substrate size studied at high resolution, J. Physiol. 570 (2006) 485–499.
[33] A. Paire, F. Bernier-Valentin, S. Selmi-Ruby, B. Rousset, Characterization of the rat thyroid iodide transporter using anti-peptide antibodies. Relationship between its expression and activity, J. Biol. Chem. 272 (1997) 18245–18249.
[34] O. Levy, A. De la Vieja, C.S. Ginter, C. Riedel, G. Dai, N. Carrasco, N-linked glycosylation of the thyroid Na^+/I^- symporter (NIS). Implications for its secondary structure model, J. Biol. Chem. 273 (1998) 22657–22663.
[35] O. Levy, G. Dai, C. Riedel, C.S. Ginter, E.M. Paul, A.N. Lebowitz, N. Carrasco, Characterization of the thyroid Na^+/I^- symporter with an anti-COOH terminus antibody, Proc. Natl. Acad. Sci. U. S. A. 94 (1997) 5568–5573.
[36] D.D. Vadysirisack, E.S. Chen, Z. Zhang, M.D. Tsai, G.D. Chang, S.M. Jhiang, Identification of in vivo phosphorylation sites and their functional significance in the sodium iodide symporter, J. Biol. Chem. 282 (2007) 36820–36828.
[37] S. Faham, A. Watanabe, G.M. Besserer, D. Cascio, A. Specht, B.A. Hirayama, E.M. Wright, J. Abramson, The crystal structure of a sodium galactose transporter reveals mechanistic insights into Na^+/sugar symport, Science 321 (2008) 810–814.
[38] A. Watanabe, S. Choe, V. Chaptal, J.M. Rosenberg, E.M. Wright, M. Grabe, J. Abramson, The mechanism of sodium and substrate release from the binding pocket of vSGLT, Nature 468 (2010) 988–991.
[39] L.M. Veenhoff, E.H. Heuberger, B. Poolman, Quaternary structure and function of transport proteins, Trends Biochem. Sci. 27 (2002) 242–249.
[40] H.H. Sitte, H. Farhan, J.A. Javitch, Sodium-dependent neurotransmitter transporters: oligomerization as a determinant of transporter function and trafficking, Mol. Interv. 4 (2004) 38–47.
[41] M.R. Castro, E.R. Bergert, T.G. Beito, P.C. Roche, S.C. Ziesmer, S.M. Jhiang, J.R. Goellner, J.C. Morris, Monoclonal antibodies against the human sodium iodide symporter: utility for immunocytochemistry of thyroid cancer, J. Endocrinol. 163 (1999) 495–504.

[42] I. Peyrottes, V. Navarro, A. Ondo-Mendez, D. Marcellin, L. Bellanger, R. Marsault, S. Lindenthal, F. Ettore, J. Darcourt, T. Pourcher, Immunoanalysis indicates that the sodium iodide symporter is not overexpressed in intracellular compartments in thyroid and breast cancers, Eur. J. Endocrinol. 160 (2009) 215–225.

[43] M. Dayem, C. Basquin, V. Navarro, P. Carrier, R. Marsault, P. Chang, S. Huc, E. Darrouzet, S. Lindenthal, T. Pourcher, Comparison of expressed human and mouse sodium/iodide symporters reveals differences in transport properties and subcellular localization, J. Endocrinol. 197 (2008) 95–109.

[44] S. Huc-Brandt, D. Marcellin, F. Graslin, O. Averseng, L. Bellanger, P. Hivin, E. Quemeneur, C. Basquin, V. Navarro, T. Pourcher, E. Darrouzet, Characterisation of the purified human sodium/iodide symporter reveals that the protein is mainly present in a dimeric form and permits the detailed study of a native C-terminal fragment, Biochim. Biophys. Acta 1808 (2011) 65–77.

[45] C. Spitzweg, C.M. Dutton, M.R. Castro, E.R. Bergert, J.R. Goellner, A.E. Heufelder, J.C. Morris, Expression of the sodium iodide symporter in human kidney, Kidney Int. 59 (2001) 1013–1023.

[46] S.M. Kaminsky, O. Levy, M.T. Garry, N. Carrasco, Inhibition of the Na^+/I^- symporter by harmaline and 3-amino-1-methyl-5H-pyrido(4,3-b)indole acetate in thyroid cells and membrane vesicles, Eur. J. Biochem. 200 (1991) 203–207.

[47] C. Gerard, V. Rigot, C. Penel, Chloride channel blockers inhibit the Na^+/I^- symporter in thyroid follicles in culture, Biochem. Biophys. Res. Commun. 204 (1994) 1265–1271.

[48] L. Vroye, R. Beauwens, J. Van Sande, D. Daloze, J.C. Braekman, P.E. Golstein, The Na^+-I^- cotransporter of the thyroid: characterisation of new inhibitors, Pflugers Arch. 435 (1998) 259–266.

[49] N. Lecat-Guillet, Y. Ambroise, Discovery of aryltrifluoroborates as potent sodium/iodide symporter (NIS) inhibitors, ChemMedChem 3 (2008) 1207–1209.

[50] N. Lecat-Guillet, G. Merer, R. Lopez, T. Pourcher, B. Rousseau, Y. Ambroise, A 96-well automated radioiodide uptake assay for sodium/iodide symporter inhibitors, Assay Drug Dev. Technol. 5 (2007) 535–540.

[51] N. Lecat-Guillet, G. Merer, R. Lopez, T. Pourcher, B. Rousseau, Y. Ambroise, Small-molecule inhibitors of sodium iodide symporter function, Chembiochem 9 (2008) 889–895.

[52] S. Lindenthal, N. Lecat-Guillet, A. Ondo-Mendez, Y. Ambroise, B. Rousseau, T. Pourcher, Characterization of small-molecule inhibitors of the sodium iodide symporter, J. Endocrinol. 200 (2009) 357–365.

[53] P. Lacotte, C. Puente, Y. Ambroise, Synthesis and evaluation of 3,4-dihydropyrimidin-2(1H)-ones as sodium iodide symporter inhibitors, ChemMedChem (2013) 104–111.

[54] P. Lacotte, D.A. Buisson, Y. Ambroise, Synthesis, evaluation and absolute configuration assignment of novel dihydropyrimidin-2-ones as picomolar sodium iodide symporter inhibitors, Eur. J. Med. Chem. 62 (2013) 722–727.

[55] L.M. Heltemes, C.R. Hagan, E.E. Mitrofanova, R.G. Panchal, J. Guo, C.J. Link, The rat sodium iodide symporter gene permits more effective radioisotope concentration than the human sodium iodide symporter gene in human and rodent cancer cells, Cancer Gene Ther. 10 (2003) 14–22.

[56] Z. Zhang, Y.Y. Liu, S.M. Jhiang, Cell surface targeting accounts for the difference in iodide uptake activity between human Na^+/I^- symporter and rat Na^+/I^- symporter, J. Clin. Endocrinol. Metab. 90 (2005) 6131–6140.

[57] J. Reizer, A. Reizer, M.H. Saier Jr., A functional superfamily of sodium/solute symporters, Biochim. Biophys. Acta 1197 (1994) 133–166.

[58] M.A. Hediger, M.F. Romero, J.B. Peng, A. Rolfs, H. Takanaga, E.A. Bruford, The ABCs of solute carriers: physiological, pathological and therapeutic implications of human membrane transport proteins, Pflugers Arch. 447 (2004) 465–468.

[59] L. He, K. Vasiliou, D.W. Nebert, Analysis and update of the human solute carrier (SLC) gene superfamily, Hum. Genomics 3 (2009) 195–206.

[60] E.M. Wright, E. Turk, The sodium/glucose cotransport family SLC5, Pflugers Arch. 447 (2004) 510–518.

[61] E.M. Wright, Glucose transport families SLC5 and SLC50, Mol. Aspects Med. 34 (2013) 183–196.

[62] A. Diez-Sampedro, B.A. Hirayama, C. Osswald, V. Gorboulev, K. Baumgarten, C. Volk, E.M. Wright, H. Koepsell, A glucose sensor hiding in a family of transporters, Proc. Natl. Acad. Sci. U. S. A. 100 (2003) 11753–11758.

[63] F.D. de Carvalho, M. Quick, Surprising substrate versatility in SLC5A6: Na^+-coupled I^- transport by the human Na^+/multivitamin transporter (hSMVT), J. Biol. Chem. 286 (2011) 131–137.

[64] D.D. Loo, T. Zeuthen, G. Chandy, E.M. Wright, Cotransport of water by the Na^+/glucose cotransporter, Proc. Natl. Acad. Sci. U. S. A. 93 (1996) 13367–13370.

[65] D.W. Leung, D.D. Loo, B.A. Hirayama, T. Zeuthen, E.M. Wright, Urea transport by cotransporters, J. Physiol. 528 (Pt 2) (2000) 251–257.

[66] M. Panayotova-Heiermann, E.M. Wright, Mapping the urea channel through the rabbit $Na^{(+)}$-glucose cotransporter SGLT1, J. Physiol. 535 (2001) 419–425.

[67] E.M. Wright, D.D. Loo, B.A. Hirayama, E. Turk, Surprising versatility of Na^+–glucose cotransporters: SLC5, Physiology (Bethesda) 19 (2004) 370–376.

[68] D.D. Loo, B.A. Hirayama, A.K. Meinild, G. Chandy, T. Zeuthen, E.M. Wright, Passive water and ion transport by cotransporters, J. Physiol. 518 (Pt 1) (1999) 195–202.

[69] E. Turk, O. Kim, J. le Coutre, J.P. Whitelegge, S. Eskandari, J.T. Lam, M. Kreman, G. Zampighi, K.F. Faull, E.M. Wright, Molecular characterization of *Vibrio parahaemolyticus* vSGLT: a model for sodium-coupled sugar cotransporters, J. Biol. Chem. 275 (2000) 25711–25716.

[70] J. Abramson, E.M. Wright, Structure and function of $Na^{(+)}$-symporters with inverted repeats, Curr. Opin. Struct. Biol. 19 (2009) 425–432.

[71] C. Wegener, S. Tebbe, H.J. Steinhoff, H. Jung, Spin labeling analysis of structure and dynamics of the $Na^{(+)}$/proline transporter of *Escherichia coli*, Biochemistry 39 (2000) 4831–4837.

[72] B.A. Hirayama, D.D. Loo, A. Diez-Sampedro, D.W. Leung, A.K. Meinild, M. Lai-Bing, E. Turk, E.M. Wright, Sodium-dependent reorganization of the sugar-binding site of SGLT1, Biochemistry 46 (2007) 13391–13406.

[73] T. Puntheeranurak, M. Kasch, X. Xia, P. Hinterdorfer, R.K. Kinne, Three surface subdomains form the vestibule of the Na^+/glucose cotransporter SGLT1, J. Biol. Chem. 282 (2007) 25222–25230.

[74] M. Quick, H. Jung, Aspartate 55 in the Na^+/proline permease of *Escherichia coli* is essential for Na^+-coupled proline uptake, Biochemistry 36 (1997) 4631–4636.

[75] T. Pirch, M. Quick, M. Nietschke, M. Langkamp, H. Jung, Sites important for Na^+ and substrate binding in the Na^+/proline transporter of *Escherichia coli*, a member of the Na^+/solute symporter family, J. Biol. Chem. 277 (2002) 8790–8796.

[76] M. Raba, T. Baumgartner, D. Hilger, K. Klempahn, T. Hartel, K. Jung, H. Jung, Function of transmembrane domain IX in the Na^+/proline transporter PutP, J. Mol. Biol. 382 (2008) 884–893.

[77] T. Liu, B. Lo, P. Speight, M. Silverman, Transmembrane IV of the high-affinity sodium-glucose cotransporter participates in sugar binding, Am. J. Physiol. Cell Physiol. 295 (2008) C64–C72.

[78] B. Wimmer, M. Raja, P. Hinterdorfer, H.J. Gruber, R.K. Kinne, C-terminal loop 13 of Na^+/glucose cotransporter 1 contains both stereospecific and non-stereospecific sugar interaction sites, J. Biol. Chem. 284 (2009) 983–991.

[79] C. Spitzweg, J.C. Morris, Genetics and phenomics of hypothyroidism and goiter due to NIS mutations, Mol. Cell. Endocrinol. 322 (2010) 56–63.

[80] J. Pohlenz, G. Medeiros-Neto, J.L. Gross, S.P. Silveiro, M. Knobel, S. Refetoff, Hypothyroidism in a Brazilian kindred due to iodide trapping defect caused by a homozygous mutation in the sodium/iodide symporter gene, Biochem. Biophys. Res. Commun. 240 (1997) 488–491.

[81] J. Pohlenz, I.M. Rosenthal, R.E. Weiss, S.M. Jhiang, C. Burant, S. Refetoff, Congenital hypothyroidism due to mutations in the sodium/iodide symporter. Identification of a nonsense mutation producing a downstream cryptic 3′ splice site, J. Clin. Invest. 101 (1998) 1028–1035.

[82] S. Kosugi, H. Okamoto, A. Tamada, F. Sanchez-Franco, A novel peculiar mutation in the sodium/iodide symporter gene in Spanish siblings with iodide transport defect, J. Clin. Endocrinol. Metab. 87 (2002) 3830–3836.

[83] M. Tonacchera, P. Agretti, G. de Marco, R. Elisei, A. Perri, E. Ambrogini, M. De Servi, C. Ceccarelli, P. Viacava, S. Refetoff, C. Panunzi, M.L. Bitti, P. Vitti, L. Chiovato, A. Pinchera, Congenital hypothyroidism due to a new deletion in the sodium/iodide symporter protein, Clin. Endocrinol. (Oxf) 59 (2003) 500–506.

[84] J.A. Liang, C.P. Chen, S.J. Huang, T.Y. Ho, C.Y. Hsiang, H.J. Ding, S.L. Wu, A novel loss-of-function deletion in sodium/iodide symporter gene in follicular thyroid adenoma, Cancer Lett. 230 (2005) 65–71.

[85] L. Montanelli, P. Agretti, G. Marco, B. Bagattini, C. Ceccarelli, F. Brozzi, T. Lettiero, M. Cerbone, P. Vitti, M. Salerno, A. Pinchera, M. Tonacchera, Congenital hypothyroidism and late-onset goiter: identification and characterization of a novel mutation in the sodium/iodide symporter of the proband and family members, Thyroid 19 (2009) 1419–1425.

[86] A. Matsuda, S. Kosugi, A homozygous missense mutation of the sodium/iodide symporter gene causing iodide transport defect, J. Clin. Endocrinol. Metab. 82 (1997) 3966–3971.

[87] S. Kosugi, S. Inoue, A. Matsuda, S.M. Jhiang, Novel, missense and loss-of-function mutations in the sodium/iodide symporter gene causing iodide transport defect in three Japanese patients, J. Clin. Endocrinol. Metab. 83 (1998) 3373–3376.

[88] S. Kosugi, S. Bhayana, H.J. Dean, A novel mutation in the sodium/iodide symporter gene in the largest family with iodide transport defect, J. Clin. Endocrinol. Metab. 84 (1999) 3248–3253.

[89] H. Fujiwara, K. Tatsumi, S. Tanaka, M. Kimura, O. Nose, N. Amino, A novel V59E missense mutation in the sodium iodide symporter gene in a family with iodide transport defect, Thyroid 10 (2000) 471–474.

[90] G. Szinnai, S. Kosugi, C. Derrien, N. Lucidarme, V. David, P. Czernichow, M. Polak, Extending the clinical heterogeneity of iodide transport defect (ITD): a novel mutation R124H of the sodium/iodide symporter gene and review of genotype–phenotype correlations in ITD, J. Clin. Endocrinol. Metab. 91 (2006) 1199–1204.

[91] M.D. Reed-Tsur, A. De la Vieja, C.S. Ginter, N. Carrasco, Molecular characterization of V59E NIS, a Na^+/I^- symporter mutant that causes congenital I^- transport defect, Endocrinology 149 (2008) 3077–3084.

[92] M. Paroder-Belenitsky, M.J. Maestas, O. Dohan, J.P. Nicola, A. Reyna-Neyra, A. Follenzi, E. Dadachova, S. Eskandari, L.M. Amzel, N. Carrasco, Mechanism of anion selectivity and stoichiometry of the Na^+/I^- symporter (NIS), Proc. Natl. Acad. Sci. U. S. A. 108 (2011) 17933–17938.

[93] V. Paroder, J.P. Nicola, C.S. Ginter, N. Carrasco, The iodide transport defect-causing mutation R124H: a delta-amino group at position 124 is critical for maturation and trafficking of the Na^+/I^- symporter (NIS), J. Cell Sci. 126 (2013) 3305–3313.

[94] A. De La Vieja, C.S. Ginter, N. Carrasco, The Q267E mutation in the sodium/iodide symporter (NIS) causes congenital iodide transport defect (ITD) by decreasing the NIS turnover number, J. Cell Sci. 117 (2004) 677–687.

[95] O. Levy, C.S. Ginter, A. De la Vieja, D. Levy, N. Carrasco, Identification of a structural requirement for thyroid Na^+/I^- symporter (NIS) function from analysis of a mutation that causes human congenital hypothyroidism, FEBS Lett. 429 (1998) 36–40.

[96] A. De la Vieja, M.D. Reed, C.S. Ginter, N. Carrasco, Amino acid residues in transmembrane segment IX of the Na^+/I^- symporter play a role in its Na^+ dependence and are critical for transport activity, J. Biol. Chem. 282 (2007) 25290–25298.

[97] O. Dohan, M.V. Gavrielides, C. Ginter, L.M. Amzel, N. Carrasco, $Na^{(+)}/I^{(-)}$ symporter activity requires a small and uncharged amino acid residue at position 395, Mol. Endocrinol. 16 (2002) 1893–1902.

[98] W. Li, J.P. Nicola, L.M. Amzel, N. Carrasco, Asn441 plays a key role in folding and function of the Na^+/I^- symporter (NIS), FASEB J. 27 (2013) 3229–3238.

[99] A. De la Vieja, C.S. Ginter, N. Carrasco, Molecular analysis of a congenital iodide transport defect: G543E impairs maturation and trafficking of the Na^+/I^- symporter, Mol. Endocrinol. 19 (2005) 2847–2858.
[100] S.L. Wu, T.Y. Ho, J.A. Liang, C.Y. Hsiang, Histidine residue at position 226 is critical for iodide uptake activity of human sodium/iodide symporter, J. Endocrinol. 199 (2008) 213–219.
[101] C.C. Li, T.Y. Ho, C.H. Kao, S.L. Wu, J.A. Liang, C.Y. Hsiang, Conserved charged amino acid residues in the extracellular region of sodium/iodide symporter are critical for iodide transport activity, J. Biomed. Sci. 17 (2010) 89.
[102] D. Russo, G. Damante, E. Puxeddu, C. Durante, S. Filetti, Epigenetics of thyroid cancer and novel therapeutic targets, J. Mol. Endocrinol. 46 (2011) R73–R81.
[103] T. Kogai, T. Endo, T. Saito, A. Miyazaki, A. Kawaguchi, T. Onaya, Regulation by thyroid-stimulating hormone of sodium/iodide symporter gene expression and protein levels in FRTL-5 cells, Endocrinology 138 (1997) 2227–2232.
[104] C. Riedel, O. Levy, N. Carrasco, Post-transcriptional regulation of the sodium/iodide symporter (NIS) by thyrotropin, J. Biol. Chem. 276 (2001) 21458–21463.
[105] P.H. Eng, G.R. Cardona, S.L. Fang, M. Previti, S. Alex, N. Carrasco, W.W. Chin, L.E. Braverman, Escape from the acute Wolff–Chaikoff effect is associated with a decrease in thyroid sodium/iodide symporter messenger ribonucleic acid and protein, Endocrinology 140 (1999) 3404–3410.
[106] P.H. Eng, G.R. Cardona, M.C. Previti, W.W. Chin, L.E. Braverman, Regulation of the sodium iodide symporter by iodide in FRTL-5 cells, Eur. J. Endocrinol. 144 (2001) 139–144.
[107] O. Dohan, Z. Baloch, Z. Banrevi, V. Livolsi, N. Carrasco, Rapid communication: predominant intracellular overexpression of the $Na^{(+)}/I^{(-)}$ symporter (NIS) in a large sampling of thyroid cancer cases, J. Clin. Endocrinol. Metab. 86 (2001) 2697–2700.
[108] I.L. Wapnir, M. van de Rijn, K. Nowels, P.S. Amenta, K. Walton, K. Montgomery, R.S. Greco, O. Dohan, N. Carrasco, Immunohistochemical profile of the sodium/iodide symporter in thyroid, breast, and other carcinomas using high density tissue microarrays and conventional sections, J. Clin. Endocrinol. Metab. 88 (2003) 1880–1888.
[109] T. Kogai, S. Sajid-Crockett, L.S. Newmarch, Y.Y. Liu, G.A. Brent, Phosphoinositide-3-kinase inhibition induces sodium/iodide symporter expression in rat thyroid cells and human papillary thyroid cancer cells, J. Endocrinol. 199 (2008) 243–252.
[110] K.A. Knostman, J.A. McCubrey, C.D. Morrison, Z. Zhang, C.C. Capen, S.M. Jhiang, PI3K activation is associated with intracellular sodium/iodide symporter protein expression in breast cancer, BMC Cancer 7 (2007) 137.
[111] D.D. Vadysirisack, A. Venkateswaran, Z. Zhang, S.M. Jhiang, MEK signaling modulates sodium iodide symporter at multiple levels and in a paradoxical manner, Endocr. Relat. Cancer 14 (2007) 421–432.
[112] Z. Zhang, S. Beyer, S.M. Jhiang, MEK inhibition leads to lysosome-mediated Na^+/I^- symporter protein degradation in human breast cancer cells, Endocr. Relat. Cancer 20 (2013) 241–250.
[113] D.K. Marsee, A. Venkateswaran, H. Tao, D. Vadysirisack, Z. Zhang, D.D. Vandre, S.M. Jhiang, Inhibition of heat shock protein 90, a novel RET/PTC1-associated protein, increases radioiodide accumulation in thyroid cells, J. Biol. Chem. 279 (2004) 43990–43997.
[114] V.E. Smith, M.L. Read, A.S. Turnell, R.J. Watkins, J.C. Watkinson, G.D. Lewy, J.C. Fong, S.R. James, M.C. Eggo, K. Boelaert, J.A. Franklyn, C.J. McCabe, A novel mechanism of sodium iodide symporter repression in differentiated thyroid cancer, J. Cell Sci. 122 (2009) 3393–3402.
[115] C. Lacoste, J. Herve, M. Bou Nader, A. Dos Santos, N. Moniaux, Y. Valogne, R. Montjean, O. Dorseuil, D. Samuel, D. Cassio, C. Portulano, N. Carrasco, C. Brechot, J. Faivre, Iodide transporter NIS regulates cancer cell motility and invasiveness by interacting with the Rho guanine nucleotide exchange factor LARG, Cancer Res. 72 (2012) 5505–5515.
[116] J. Wolff, Transport of iodide and other anions in the thyroid gland, Physiol. Rev. 44 (1964) 45–90.
[117] J. Di Bernardo, C. Iosco, K.J. Rhoden, Intracellular anion fluorescence assay for sodium/iodide symporter substrates, Anal. Biochem. 415 (2011) 32–38.
[118] M. Tonacchera, A. Pinchera, A. Dimida, E. Ferrarini, P. Agretti, P. Vitti, F. Santini, K. Crump, J. Gibbs, Relative potencies and additivity of perchlorate, thiocyanate, nitrate, and iodide on the inhibition of radioactive iodide uptake by the human sodium iodide symporter, Thyroid 14 (2004) 1012–1019.
[119] A. Yoshida, N. Sasaki, A. Mori, S. Taniguchi, Y. Mitani, Y. Ueta, K. Hattori, R. Sato, I. Hisatome, T. Mori, C. Shigemasa, S. Kosugi, Different electrophysiological character of I^-, ClO_4^-, and SCN^- in the transport by Na^+/I^- symporter, Biochem. Biophys. Res. Commun. 231 (1997) 731–734.
[120] M.A. Larkin, G. Blackshields, N.P. Brown, R. Chenna, P.A. McGettigan, H. McWilliam, F. Valentin, I.M. Wallace, A. Wilm, R. Lopez, J.D. Thompson, T.J. Gibson, D.G. Higgins, ClustalW and ClustalX version 2, Bioinformatics 23 (2007) 2947–2948.
[121] J. Pohlenz, L. Duprez, R.E. Weiss, G. Vassart, S. Refetoff, S. Costagliola, Failure of membrane targeting causes the functional defect of two mutant sodium iodide symporters, J. Clin. Endocrinol. Metab. 85 (2000) 2366–2369.
[122] S.W. Chen, J.L. Pellequer, Identification of functionally important residues in proteins using comparative models, Curr. Med. Chem. 11 (2004) 595–605.
[123] O. Pible, G. Imbert, J.L. Pellequer, INTERALIGN: interactive alignment editor for distantly related protein sequences, Bioinformatics 21 (2005) 3166–3167.
[124] J.L. Pellequer, A.J. Gale, E.D. Getzoff, J.H. Griffin, Three-dimensional model of coagulation factor Va bound to activated protein C, Thromb. Haemost. 84 (2000) 849–857.
[125] W. Humphrey, A. Dalke, K. Schulten, VMD: visual molecular dynamics, J. Mol. Graph. 14 (1996) 33–38(27–38).